

MULTISTEP DIRECT PROCESSES IN NEUTRON SCATTERING AT 26 MeV

ANDRZEJ MARCINKOWSKI[†]

The Andrzej Soltan Institute for Nuclear Studies
Hoża 69, 00-681 Warszawa, Poland

AND PARASKEVI DEMETRIOU

Institute d'Astrophysique et d'Astronomie, Université Libre de Bruxelles
CP-226 Campus La Plaine, B-1050 Brussels, Belgium

(Received September 9, 2003)

The contributions of multistep direct reactions with different sequences of the leading continuum nucleons are presented for neutron scattering by niobium at incident energy of 26 MeV. The multistep cross sections are calculated within the framework of the Feshbach, Kerman and Koonin theory using non-DWBA matrix elements. The one-step cross sections include excitations of both incoherent particle-hole pairs and coherent collective vibrations. The results show that the dominant sequences involve only neutrons in the continuum, while sequences involving protons can be neglected.

PACS numbers: 25.40.Fq, 24.60.Gv

1. Introduction

The multistep direct (MSD) reaction theory of Feshbach, Kerman and Koonin (FKK) [1] has been widely used to describe nucleon induced reactions in the continuum. This is mainly due to its appealing convolution structure that makes the calculation of higher order cross sections feasible. In recent works the formulation of the MSD cross section with non-DWBA matrix elements has been applied extensively to the analysis of nucleon scattering and charge-exchange reactions [2-8]. The enhanced MSD cross sections including the non-DWBA matrix elements have proved to be sufficient to compensate for the reduction of the one-step (1SD) cross sections imposed

[†] Send any remarks to Andrzej.Marcinkowski@fuw.edu.pl

by the energy weighted sum rules (EWSR). The 1SD cross sections include contributions from the excitation of one-phonon collective states (vib) of multipolarity $\lambda \leq 4$ and from the incoherent excitation of particle-hole pairs (ph) with orbital angular momenta reduced to $L > 4$ only, both satisfying the EWSR's limits [9,10]. It has been also shown that the MSD reaction includes more than one sequence of M successive two-body collisions between the leading continuum particle (being either a proton or a neutron) and the bound nucleons of the target [6–8,11]. The relative contributions of these sequences depend on the available energy and on the type of nucleons in each of the two-body collisions, *i.e.* whether the collision involves a (pp), (nn), (np) or (pn) reaction stage. So far in the literature [2–5,12–15], only collisions resulting in M successive neutron scattering (nn) stages were taken into account in the MSD cross sections for inelastic scattering of neutrons. The novelty of the present paper lies in the fact that all multistep sequences of the intranuclear reaction stages that contribute to the MSD cross section for neutron scattering are calculated for the first time. Thus, the aim of this paper is to corroborate or deny the commonly used assumption of the negligence of sequences including protons. The calculations are done for the $^{93}\text{Nb}(n, n')^{93}\text{Nb}$ reaction at 26 MeV.

2. The non-DWBA matrix elements in the MSD formalism

According to the FKK theory, the cross section for a multistep direct reaction is obtained by multiple convolution of one-step 1SD cross sections [1,16],

$$\begin{aligned} \left(\frac{d^2\sigma}{dE d\Omega} \right)_{\text{MSD}} &= \int \frac{m_1 E_1}{(2\pi)^2 \hbar^2} dE_1 d\Omega_1 \\ &\times \int \frac{m_2 E_2}{(2\pi)^2 \hbar^2} dE_2 d\Omega_2 \dots \int \frac{m_{M-1} E_{M-1}}{(2\pi)^2 \hbar^2} dE_{M-1} d\Omega_{M-1} \\ &\times \left(\frac{d^2\sigma}{dE_M d\Omega_M} \right)_{\text{1SD}} \dots \left(\frac{d^2\sigma}{dE_2 d\Omega_2} \right)_{\text{1SD}} \left(\frac{d^2\sigma}{dE_1 d\Omega_1} \right)_{\text{1SD}}. \end{aligned} \quad (1)$$

E_M , m_M and Ω_M are the energy, mass and the solid angle of the scattered nucleon after the M -th stage of the reaction. In practical calculations one assumes that the final states in the incoherent (ph) component of the 1SD cross section are those of the particle-hole just created, independent on the reaction stage M . Thus, the particles and holes excited at the preceding stages act as spectators only. On the other hand, each phonon in the coherent collective (vib) term of the 1SD cross section, in Eq. (1), results in multi-phonon states [17] built on the final phonon states of the preceding reaction stage. Therefore it is important to include only one-phonon states in the collective component of the 1SD cross section.

The cross sections describing the successive transitions, in Eq. (1), include, apart from the last one, the non-DWBA matrix elements. The latter are a result of biorthogonality of the distorted waves [18]. These non-DWBA matrix elements can be obtained by multiplying each partial l -component of the incoming distorted wave in the DWBA matrix element by the inverse elastic S_l -matrix element [19]. One immediate consequence is that the non-DWBA matrix elements are larger than the normal ones. Enhanced are both the incoherent $1p1h$ -pairs as well as those pairs that add coherently to the collective vibrations, since the distorted waves, whether the excited states are single-particle ones or collective, are the same eigenfunctions of the complex optical potential and form a complete set with the adjoint distorted waves.

For any transfer of multipolarity λ or orbital angular momentum L , a number of partial waves l_{M-1}, l_{M-2} contribute to the incoming and outgoing distorted waves (triangle rule), respectively. The incoming waves in the outgoing channel ($M-1$) are just enhanced by the inverse elastic scattering matrix elements $|S_{l_{M-1}}|^{-1}$. However, these enhancing factors are too large at incident energies higher than 50 MeV, and provide divergent MSD cross sections [2,7]. Smaller enhancing factors are expected to result from energy averaging in the continuum [10]. On the other hand, in the theory of FKK the enhanced transition matrix elements are averaged over energy. To obtain the energy average we approximate the net effect of the different averaged enhancing factors $\langle |S_{l_{M-1}}| \rangle^{-1}$, acting on each partial wave l_{M-1} for a specific L , by an average enhancing factor $\langle |S_L| \rangle^{-1}$. The elastic scattering matrix elements are expressed in terms of the partial wave transmission coefficients of the optical model T_L , $|S_L|^2 = 1 - T_L$. The energy averaging of $\langle |S_L| \rangle^{-1}$ makes the enhancing factors smooth and free of singularities that arise at the energies of the single-particle resonances, when the transmission coefficients T_L 's approach unity. In practice, such anomalies were removed by adopting an average dependence of the respective T_L on energy [10].

Following [10] the 1SD cross section for neutron scattering reads,

$$\begin{aligned}
 \left(\frac{d^2\sigma}{dE d\Omega} \right)_{\text{1SD}} = & \sum_{\lambda \leq 4, \tau=0,1} \frac{1}{4} (1 + 3\delta_{0,\tau}) \beta_{\lambda,\tau}^2 \left(\frac{d\sigma}{d\Omega} \right)_{\lambda,\tau}^{\text{DWBA-macr}} f[\hbar\omega_{\lambda,\tau}, I] \\
 & + \sum_{L>4} (2L+1)P \times \omega_{1p\pi 1h\pi}(U, \varepsilon_F^\pi) \times R_{1,1}(L) V_{\pi,\nu}^2 \left\langle \left(\frac{d\sigma}{d\Omega} \right)_{1p\pi 1h\pi(L)}^{\text{DWBA-micr}} \right\rangle \\
 & + \sum_{L>4} (2L+1)P \times \omega_{1p\nu 1h\nu}(U, \varepsilon_F^\nu) \times R_{1,1}(L) V_{\nu,\nu}^2 \left\langle \left(\frac{d\sigma}{d\Omega} \right)_{1p\nu 1h\nu(L)}^{\text{DWBA-micr}} \right\rangle, \quad (2)
 \end{aligned}$$

and for (p, n) reactions,

$$\begin{aligned} \left(\frac{d^2\sigma}{dEd\Omega} \right)_{1SD} &= \sum_{\lambda \leq 4} \frac{1}{2} \beta_{\lambda,1}^2 \left(\frac{d\sigma}{d\Omega} \right)_{\lambda,1}^{\text{DWBA-macr}} f[\hbar\omega_{\lambda,1}, \Gamma] \\ &+ \sum_{L>4} (2L+1)P \times \omega_{1p_\pi 1h_\nu}(U, \varepsilon_F^\nu) \times R_{1,1}(L) V_{\pi,\nu}^2 \left\langle \left(\frac{d\sigma}{d\Omega} \right)_{1p_\pi 1h_\nu(L)}^{\text{DWBA-micr}} \right\rangle. \end{aligned} \quad (3)$$

For proton scattering, $V_{\pi,\nu}$ and $V_{\nu,\nu}$ in (2) are exchanged for $V_{\pi,\pi}$ and $V_{\pi,\nu}$, respectively, while for the (n, p) reactions $1p_\pi 1h_\nu$ and ε_F^ν in (3) are swapped with $1p_\nu 1h_\pi$ and ε_F^π , respectively (see, *e.g.* [7,10]). The first term in (2) describes the isoscalar one-phonon collective (vib) cross sections and the two following terms describe the incoherent particle-hole (ph) cross sections for the excitation of proton and neutron ph -pairs, respectively. The cross sections of the charge-exchange (pn) and (np) reaction stages are calculated in an approximate way described in the Section 3.

Thus, $(M-1)$ out of the M 1SD cross sections, in Eq. (1), contain a sum of the enhanced (vib S^{-2}) = $\sum_{\lambda \leq 4} \sigma_\lambda(\text{vib}) \langle S_\lambda \rangle^{-2}$ and ($ph S^{-2}$) = $\sum_{L>4} \sigma_L(ph) \langle S_L \rangle^{-2}$ cross sections. As a result the multistep cross section of Eq. (1) includes the following combinations of the two terms [4,5,12]:

1SD, (vib) + (ph);

2SD, (vib S^{-2} , vib) + ($ph S^{-2}$, vib) + (vib S^{-2} , ph) + ($ph S^{-2}$, ph);

3SD, *etc.*

The factors S^{-2} act in the outgoing channels (on incoming distorted waves). However, in the multistep approach we use, the leading particle in the continuum does not have to be the same throughout the scattering sequence and this leads to different sequences of reaction stages. Therefore, the one-phonon (vib) and the (ph) components are lumped into the 1SD cross sections for the (nn), (pp), (pn) and (np) reaction stages that are used, in Eq. (1), repeatedly in the sequences of the M reaction stages that contribute to the MSD reaction considered. In the case of neutron scattering all the sequences are listed in Table I, where we have used the abbreviation $(nn S^{-2}) = \sum_L \sigma_L(n, n') \langle S_L \rangle^{-2}$. One can see that in order to obtain the MSD cross sections for inelastic scattering of neutrons $^{93}\text{Nb}(n, n')^{93}\text{Nb}$, one also has to calculate the 1SD cross sections in the remaining reaction channels; $^{93}\text{Zr}(p, p')^{93}\text{Zr}$, $^{93}\text{Zr}(p, n)^{93}\text{Nb}$ and $^{93}\text{Nb}(n, p)^{93}\text{Zr}$.

TABLE I

The decomposition of the MSD cross sections for the $^{93}\text{Nb}(n, n')^{93}\text{Nb}$ reaction at 26 MeV.

$\sigma(1\text{SD})$	(mb)	$\sigma(2\text{SD})$	(mb)	$\sigma(3\text{SD})$	(mb)
(<i>ph</i>)	214	(<i>nnS</i> ⁻² , <i>nn</i>)	215	(<i>nnS</i> ⁻² , <i>nnS</i> ⁻² , <i>nn</i>)	96
(vib)	140	(<i>npS</i> ⁻² , <i>pn</i>)	9.5	(<i>nnS</i> ⁻² , <i>npS</i> ⁻² , <i>pn</i>)	3.6
				(<i>npS</i> ⁻² , <i>pnS</i> ⁻² , <i>nn</i>)	2.4
				(<i>npS</i> ⁻² , <i>ppS</i> ⁻² , <i>pn</i>)	2.4
Total	354		224.5		104.4

3. Calculations and comparison with experiment

The (*nn*) and (*pp*) reaction stages are calculated according to Eq. (2). The macroscopic DWBA cross sections in the first, (vib) term of the r.h.s. of Eq. (2) are calculated with form factors $F_\lambda = -R\partial U/\partial R$ obtained by using the complex optical potential of [20] for neutrons and [21] for protons. The following isoscalar ($\tau=0$) one-phonon states are taken into account for ^{92}Zr : 2_1^+ at 0.93 MeV with $\beta_2=0.13$, 2_3^+ at 2.49 MeV with $\beta_2=0.08$ and 3_1^- at 2.30 MeV with $\beta_3=0.18$. The dipole, quadrupole and low energy component of the octupole (LEOR) giant resonances are also included. The LEOR exhausts 30% of the octupole strength [22]. The deformation parameters for the giant resonances are obtained by depletion of the energy weighted sum rules (EWSR's). The energy distribution function f_λ is a Gaussian type, adjusted to the experimental energy resolution for the low-energy one-phonon levels, or a Lorentzian type with width typical of the giant resonances.

The incoherent microscopic DWBA cross sections in the second and third terms of Eq. (2) are calculated using a particle-hole form factor. A real effective interaction of Yukawa form with 1 fm range and strengths $V_{\pi,\pi} = 12.7$ MeV and $V_{\pi,\nu} = 43.1$ MeV [23], depending on energy according to [24], is used. The spectroscopic amplitude $(2j_h + 1)^{1/2}$ is included. These cross sections are averaged over final states $(j_p j_h^{-1})_{LM}$ of the shell model contained in 1 MeV energy bins. When there are no states with given L transfer in the 1 MeV bin, the width of the bin is increased until at least one state is found. This approximate method allows one to include also the continuum states in the calculations using a standard DWBA code. The terms $P = 1/2$ and $R_{1,1}(L)$ in (2) are the parity and spin distributions of the $1p1h$ states. The density of the final $1p1h$ states $\omega_{1p1h_j}(U, \varepsilon_F^j)$ is given by the two-component formula of Betak and Dobes [25] with the hole-depth restriction (ε_F):

$$\omega_{1p1h_j}(U, \varepsilon_F^j) = g_i g_j [U - (U - \varepsilon_F^j)\Theta(U - \varepsilon_F^j)], \quad (4)$$

and with $i = j = \pi$ for $p_\pi = h_\pi = 1$ and $p_\nu = h_\nu = 0$; $i = j = \nu$ for $p_\nu = h_\nu = 1$ and $p_\pi = h_\pi = 0$; $i = \pi, j = \nu$ for $p_\nu = h_\pi = 0$ and $p_\pi = h_\nu = 1$; $i = \nu, j = \pi$ for $p_\pi = h_\nu = 0$ and $p_\nu = h_\pi = 1$. The Θ is the Heaviside step function. The equidistant single-particle state densities of protons and neutrons are $g_\pi = Z/13$ and $g_\nu = N/13$, respectively. The spin cutoff parameter in $R_{1,1}(L)$ is $\sigma^2 = 0.28nA^2/3$ with $n = 2$ being the number of excited particles and holes.

The deformation parameters for the weak isovector ($\tau=1$) excitations are not well known (see, *e.g.* Refs. in [22]). Therefore, we have assumed that the isovector cross sections are dominated by the giant resonances. The latter, except for the giant dipole resonance, have a broad and smooth energy dependence [22]. Bearing this in mind, we approximated the isovector cross sections to the individual collective levels by the smooth (ph)-cross sections of the second r.h.s. term of Eq. (3), calculated for $L \leq 4$. These cross sections are then reduced by applying the EWSR's. Both the macroscopic and the microscopic cross sections were calculated with the DWUCK-4 code [26].

In Fig. 1 the contributions from excitation of the one-phonon collective states (vib) and the incoherent particle-hole (ph) states are included in the 1SD cross section for the neutron scattering stage (nn). The structure at

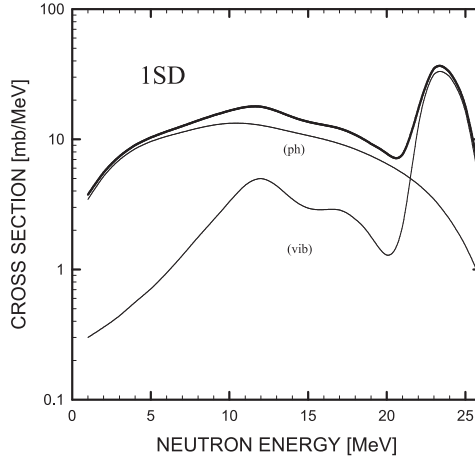


Fig. 1. The 1SD cross section of the $^{93}\text{Nb}(n, n')^{93}\text{Nb}$ reaction, at incident neutron energy of 26 MeV (thick solid line). The contributions due to one-phonon collective vibrations of multipolarity $\lambda \leq 4$ and to incoherent ph -pairs of transferred orbital angular momenta $L > 4$ are shown separately.

the highest outgoing energies corresponds to the low-energy collective states. This structure, in the case of the two-step, (nnS^{-2}, nn), and the three-step, (nnS^{-2}, nnS^{-2}, nn) sequences, appears as two-phonon and three-phonon structure at twice and thrice the excitation energy, in Figs. 2 and 3, respec-

tively. The angle- and energy-integrated cross sections for all relevant sequences of reaction stages are gathered together in Table I. From Figs. 2 and 3 and from Table I, it is evident that the sequences of collisions that include only neutron scattering (nn) stages dominate markedly over the ones that involve also protons. In the investigated case, the summed 1SD (nn), 2SD (nnS^{-2}, nn) and 3SD (nnS^{-2}, nnS^{-2}, nn) sequences give 665 mb, whereas the ones involving the charge-exchange (np) and (pn) stages or the proton scattering (pp) stage give only 18 mb. This result provides a clear evidence that the neglect of all multistep sequences involving protons in [2-5], is a justifiable approach.

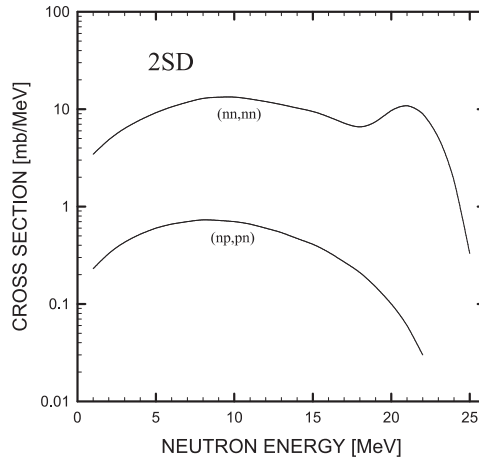


Fig. 2. The same as in Fig. 1 but for the 2SD reaction. The contributions from the two sequences of reaction stages are shown (sum of the two contributions is indistinctive from the stronger one). The enhancing factors S^{-2} are omitted for simplicity.

The contributions from the MSD processes are substantial. The integrated 2SD and 3SD neutron emission cross sections at the incident energy of 26 MeV are 225 mb and 104 mb, respectively, compared to the 354 mb of the 1SD cross section which includes the contribution of (ph)=214 mb and (vib)=140 mb.

Evaporation of low energy neutrons from the compound nucleus (CN) is calculated according to the theory of Hauser and Feshbach. The cross sections for multistep compound (MSC) emission are calculated in the framework of the theory of FKK [1,27]. Gradual absorption [3,27] of incident flux directly into the quasi-bound states of the MSC reaction chain is taken into account. The radial overlap integral of the single-particle wave functions in the MSC cross section is calculated with constant wave functions within the nuclear volume. The overlap integral is then reduced in order

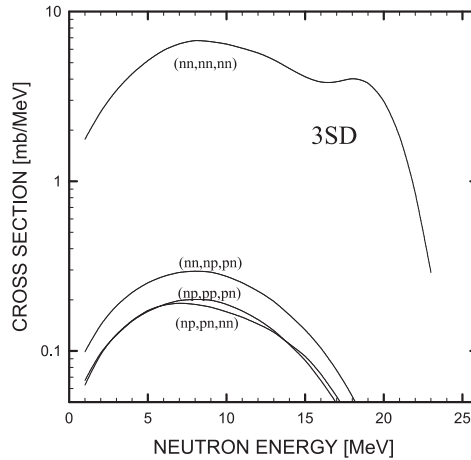


Fig. 3. The same as in Fig. 1 but for the 3SD reaction. The contributions from the four sequences of reaction stages are shown (sum of the four contributions is indistinctive from the strongest one). The enhancing factors S^{-2} are omitted for simplicity.

to approximate the result of the microscopic calculation [28]. The resulting cross sections amount to about $1/4$ of those obtained with the constant wave functions [28].

The calculated MSD-, MSC- and CN-cross sections are compared with the inclusive neutron spectrum measured at incident energy of 25.7 MeV [29], in Fig. 4. The overall agreement between theory and experiment is good over the entire energy range. Fig. 4 clearly shows how the one-phonon maximum in the 1SD spectrum develops into the two-phonon, three-phonon and four-phonon maxima at twice, trice and four times higher excitation energy in the 2SD, 3SD and 4SD spectra, respectively. This result depends quite critically on the fine integration grid, in Eq. (1), that saturates the numerical response and removes the spurious one-phonon peaks from the MSD spectra shown in Fig. 3 of Ref. [4].

It is worth noting that the contribution of the MSC reactions is insignificant in comparison with the MSD component. This is partly due to the reduced microscopic radial overlap integral applied [28] and partly to the gradual absorption [3,27].

The cross sections for the $^{93}\text{Nb}(n, xn)^{93}\text{Nb}$ reaction have also been analysed by using the basis of collective states of the RPA. Only the first two steps of the reaction were calculated in [30]. The results obtained at the incident energy of 26 MeV — 1SD = 408 mb, 2SD = 260 mb — are in satisfactory agreement with the results of the present work (see Table I). From Fig. 5 it is evident that the RPA emission spectra are also similar to

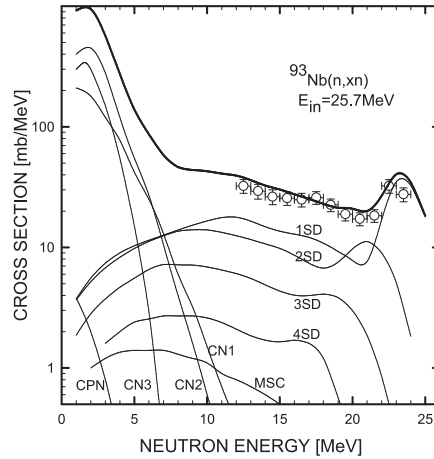


Fig. 4. Comparison of the calculated cross sections with the spectrum of neutrons from the $^{93}\text{Nb}(n,xn)^{93}\text{Nb}$ reaction measured at incident energy of 25.7 MeV [29]. The thick line is a sum of all contributions. CN1 to CN3 denote the primary, secondary and tertiary neutrons evaporated from the compound nucleus, respectively. CPN denotes secondary neutrons preceded by evaporation of a proton and MSC labels the emission from the three steps of the compound reaction.

those obtained in the present work. These results further confirm [6] that the MSD cross sections of Eq. (1), together with Eq. (2), make a closed form approach of the RPA cross sections.

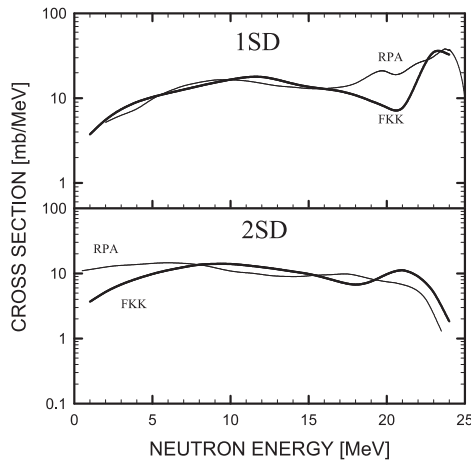


Fig. 5. Comparison of the 1SD and 2SD cross sections calculated for the $^{93}\text{Nb}(n,n')^{93}\text{Nb}$ reaction at incident energy 26 MeV (FKK) with the corresponding cross sections obtained by Lenske *et al.* [30] with use of the RPA basis states.

4. Conclusions

The enhanced MSD cross sections of the FKK theory, obtained with the 1SD cross section of [10] and the non-DWBA matrix elements, and allowing for all multistep sequences of reaction stages, reproduce the inclusive inelastic neutron scattering data measured at 25.7 MeV [29] well. The results show that at this energy the multistep sequences of successive (nn) reaction stages are by far the dominant ones and that contributions from sequences also including protons amount only to about 3% of the total. This result justifies the neglect of sequences including continuum protons in the calculations, practiced in [2–5,12–15].

Already at 26 MeV the MSD reactions dominate over the MSC ones.

REFERENCES

- [1] H. Feshbach, A. Kerman, S.E. Koonin, *Ann. Phys. (NY)* **125**, 429 (1980).
- [2] M.B. Chadwick, P.G. Young, F.S. Dietrich, Lawrence Livermore National Laboratory Report UCRL-JC-117460, June 1994; *Intermediate Energy Nucl. Data: Models and Codes*, OECD(NEA), Issy-Ies-Moulineaux, France, 1994, p.67.
- [3] G. Arbanas, M.B. Chadwick, F.S. Dietrich, A. Kerman, *Phys. Rev.* **C51**, R1078 (1995).
- [4] P. Demetriou, A. Marcinkowski, B. Mariański, *Phys. Lett.* **B493**, 281 (2000).
- [5] A. Marcinkowski, P. Demetriou, B. Mariański, *Nucl. Phys.* **A694**, 312 (2001); *APH N.S., Heavy Ion Physics* **16/1-4**, 35 (2002).
- [6] P. Demetriou, A. Marcinkowski, B. Mariański, *Acta Phys. Pol. B* **32**, 3003 (2001); *Nucl. Phys.* **A697**, 171 (2002).
- [7] P. Demetriou, A. Marcinkowski, B. Mariański, *Nucl. Phys.* **A707**, 354 (2002).
- [8] P. Demetriou, A. Marcinkowski, *Nucl. Phys.* **A714**, 75 (2003).
- [9] A. Marcinkowski, B. Mariański, *Phys. Lett.* **B433**, 223 (1998).
- [10] A. Marcinkowski, B. Mariański, *Nucl. Phys.* **A653**, 3 (1999).
- [11] A.J. Koning, M.B. Chadwick, *Phys. Rev.* **C56**, 970 (1997).
- [12] H. Kalka, *Z. Phys.* **A341**, 289 (1992).
- [13] M.B. Chadwick, P.G. Young, *Phys. Rev.* **C47**, 2255 (1993).
- [14] Y. Watanabe, A. Aoto, K. Kashimoto, S. Chiba, T. Fukatori, K. Hasegawa, M. Mizumoto, S. Meigo, M. Sugimoto, Y. Yamanouti, N. Koori, M.B. Chadwick, P.E. Hodgson, *Phys. Rev.* **C51**, 1891 (1995).
- [15] P. Demetriou, A. Marcinkowski, B. Mariański, *J. Nucl. Sci. Technol.*, Supplement 2, p. 726 (August 2002).
- [16] A. Marcinkowski, R.W. Finlay, J. Rapaport, P.E. Hodgson, M.B. Chadwick, *Nucl. Phys.* **A501**, 1 (1989).

- [17] N.A. Smirnova, N. Pietralla, T. Mizusaki, P. Van Isacker, *Nucl. Phys.* **A678**, 235 (2000).
- [18] M.S. Hussein, R. Bonetti, *Phys. Lett.* **B112**, 189 (1982).
- [19] I. Kumabe, M. Haruta, M. Hyakutake, M. Matoba, *Phys. Lett.* **B140**, 272 (1984).
- [20] D. Wilmore, P.E. Hodgson, *Nucl. Phys.* **55**, 673 (1964).
- [21] F. Bjorklund, S. Fernbach, *Phys. Rev.* **109**, 295 (1958); in Proc. Int. Conf. on Nuclear Optical Model, Florida State University Studies No 32, Tallahassee, 1959.
- [22] A. van der Woude in: ed. J. Speth, *Electric and Magnetic Giant Resonances in Nuclei*, World Scientific, Singapore 1991, p. 177.
- [23] S.M. Austin, in: eds. C.D. Goodman *et al.*, *Proc. Conf. on (p,n) Reactions and the Nucleon-Nucleon Force*, Telluride, Colorado 1979, Plenum Press, NY 1980, p. 203.
- [24] E. Gadioli, P.E. Hodgson, *Pre-Equilibrium Nuclear Reactions*, Clarendon, Oxford, 1992, p. 385.
- [25] E. Betak, J. Dobes, *Z. Phys.* **279**, 319 (1976).
- [26] P.D. Kunz, E. Rost, in: K. Langanke *et al.* (Eds.), *Computational Nuclear Physics*, Vol. 2, Springer, Berlin 1993, Ch. 5.
- [27] A. Marcinkowski, J. Rapaport, R.W. Finlay, C. Brient, M. Herman, M.B. Chadwick, *Nucl. Phys.* **A561**, 387 (1993).
- [28] T. Kawano, *Phys. Rev.* **C59**, 865 (1999); and private communication.
- [29] A. Marcinkowski, R.W. Finlay, G. Randers-Pehrson, C.E. Brient, R. Kurup, S. Mellema, A. Meigooni, R. Taylor, *Nucl. Sci. Eng.* **83**, 13 (1983).
- [30] H. Lenske, H.H. Wolter, M. Herman, G. Reffo, in: Proc. 7-th Int. Conf. on Nuclear Reaction Mechanisms, Varenna 1994, ed. E. Gadioli, *Ric. Sci. Suppl.* **100**, 110 (1994).